Electromagnetic Sensor-directed Spatio-temporal Variability of Soil Salinity in the Coastal Areas

Guo Yan[1], Shi Zhou[2], Wang Laigang[1],Cheng Yongzheng[1], Liu Ting[1]*

[1] Institute of Agricultural Economy & Information, Henan Academy of Agricultural Sciences, Zhengzhou 450002, China e-mail: 10914063@zju.edu.cn

[2] Institute of Agricultural Remote Sensing and Information Technology Application, College of Environmental and Resource Sciences, Zhejiang University, Hangzhou 310058, China e-mail: shizhou@zju.edu.cn

Abstract

Proximally sensed soil measurements have become an interesting source of auxiliary information to characterize within-field spatio-temporal variability. Some proximal sensors, such as the EM38 allows for the rapid, cost-effective collection of high-resolution data in-situ. In this study, we employed EM38 data to conduct spatio-temporal variability analysis in a coastal area. (Geo)statistics analysis was used to detect the spatio-temporal variability of soil salinity with high salinity (EM $\geqslant$175 mS m^{-1}) in the middle, low salinity (EM $\leqslant$100 mS m^{-1}) in the surroundings. The Tukey-Kramer means comparisons for ECa implied significant difference between years of ECa. Coefficient of variation over time at each measurement showed that the middle region with a high salinity content displayed temporal stability, while the surrounding region of a lower salinity level showed temporal instability. This result could be used for the division of plots into different management zones directing the farmer to plant, or scheduling the variable rate application.

1. Introduction

Proximal soil sensing (PSS) has two notable advantages over traditional methods. First, through minimal effort, they can rapidly and cost-effectively acquire soil information; secondly, they can collect enough soil data to allow meaningful geo(statistical) analyses to confirm spatial soil attributes. Recently, highly detailed soil sensor data have become an interesting source of auxiliary data to detect/characterize within-field soil variability[1]. This mainly includes electrical and electromagnetic sensors (i.e. EM38)[2], optical and radiometric sensors (i.e. ASD)[3], mechanical sensors (i.e. soil strength profile sensor)[4], electrochemical sensors (i.e. ISFETs)[5]. Of these, EM38 has the unique ability to detect soil properties (i.e. texture, water content, salinity) by measurements of soil apparent electrical conductivity (ECa) with on-the-go or stop-and-go style. As reported, ECa is mainly responded to soil salinity under saline conditions[6-7]. For instances, many scientific literatures have been well documented the relationship between ECa and soil salinity[6,8-9]. Where yield correlates with ECa, maps of ECa are useful for devising soil management or agricultural practices. In reclaimed coastal areas, soil salinity is the main factor limiting agricultural productivity. In such situations, farmers and land managers need to be able to understand and identify the spatio-temporal variability of saline areas for the sake of agricultural and economic benefits. With regard to identifying and mapping the spatio-temporal variability of soil salinity, geostatistical tools with spatially georeferences are common. For example, Douaik *et al*[10] used spatio-temporal kriging and Bayesian maximum entropy to predict soil salinity at unobserved spatial locations and time instants.

Reliable, timely, and cost-effective soil salinity monitoring and assessments are needed for an understanding of the dynamics of soil salinity spatio-temporal changes[9]. Despite this fact, there are very few publications on the spatio-temporal variability of soil properties in reclaimed coastal regions with continuous monitoring over multiple years with proximally sensed data. Hence, the main objective was to confirm the reliability of characterizing soil salinity by ECa in a coastal saline field in Zhejiang province, China. We also analyzed the spatio-temporal stability of soil salinity and mapped the temporal stability for better management with respect to soil salinity.

2. Materials and methods

2.1. Study region

The study was conducted on a 4.25 ha paddy field in a coastal saline area located in the northern region of Shangyu City, Zhejiang Province southeast of China's Hangzhou Gulf of the Yangtse delta. This covers an area of 26,061 ha (30°04'00"-30°13'47"N, 120°38'32"-120°51'53"E). The area experiences a subtropical climate with an average annual temperature of 16.5 °C and an average annual precipitation of 1300 mm. Around Shangyu city, approximately 17,000 ha of coastal land has been reclaimed over the past 40 years. The soil is therefore derived from recent marine and fluvial deposits. The investigated fields were reclaimed in 1996.

2.2. Data collection and processing

In the present study, we used the program EM38 (Geonics Ltd, Ont, Canada) proto record data (i.e. electrical conductivity) with the Geonics EM38 Data Logging System (DAS70-CX) consisting of a field computer Allegro CX. Data files created with this program were used to position a survey according to the locations recorded separately by a Global Positioning System (GPS). Such results can be combined with EM38 records through NMEA-0183 compatible data[11]. Time series ECa data were collected by EM38 sensor in October 2009, November 2010 and November 2011 along the furrows with GPS.

978-1-4673-5225-3/14/$31.00 ©2014 IEEE

2.3. Spatio-temporal variability analysis

Geostatistical approaches are often used to define the variance structure, spatial distribution and trend changes of soil. The spatial variance of ECa is interpolated by ordinary kriging (OK)[12]. With regard to the temporal stability, we calculated the coefficient of variation (CVt_i) over time at each measurement to assess the stability of soil salinity by ECa. The technique has been used by Blackmore[13] to assess the temporal stability of crop yields and by Shi *et al*[14] to assess the soil properties in grasslands.

$$CVt_i = \frac{\sqrt{(n\times\sum_{t=1}^{n}\mathrm{ECa}_{it}{}^{2} - (\sum_{i=1}^{n}\mathrm{ECa}_{it})^{2})/n\times(n-1)}}{(\sum_{i=1}^{n}\mathrm{ECa}_{it})/n}$$

Where CVt_i is the coefficient of variation over time at the ith ECa measurement location in the tth time; n is the number of ECa.

3. Results and discussions

3.1. Statistical analysis of multi-temporal EM38 data

Table 1 shows some basic summary statistics and quartile estimates for soil electrical conductivity measured by EM38 sensor in 2009, 2010 and 2011. The average values show decreasing trend substantially from 2009 (i.e. 166.19 mS m^{-1}) to 2010 (i.e. 134.02 mS m^{-1}) with a less decrease from 2010 to 2011 (i.e. 20.73 mS m^{-1}). The quartile estimates show a decreasing trend from 2009 to 2011, with a lesser difference between 2010 and 2011 than 2009 and 2010. Fig. 1a gives the curve of the cumulative distribution function (CDF) for our study site which shows visible variations among the three years. That is, for a given ECa value, the CDF was largest in 2009 and least in 2011. In order to validate the differences, we chose the Tukey-Kramer multiple comparison procedure. Fig. 1b shows the plot of the calculated Tukey-Kramer means comparisons for ECa, and the Tukey-Kramer means comparisons are shown in Table 2. The values indicate the actual absolute differences in the means minus the least significant difference (i.e. abs-LSD). Here, there are two important things to note, first, that the mean with positive values indicates significant difference, and second, because the borders of the table are sorted by the mean, the most significant differences among the years appear in the upper right hand corner. As shown in Table 2, ECa is significantly different between 2009, 2010, and 2011. That is, ECa is significantly different for 2009 and 2011 (42.06), 2009 and 2010 (22.71). These are shown in Fig. 1b.

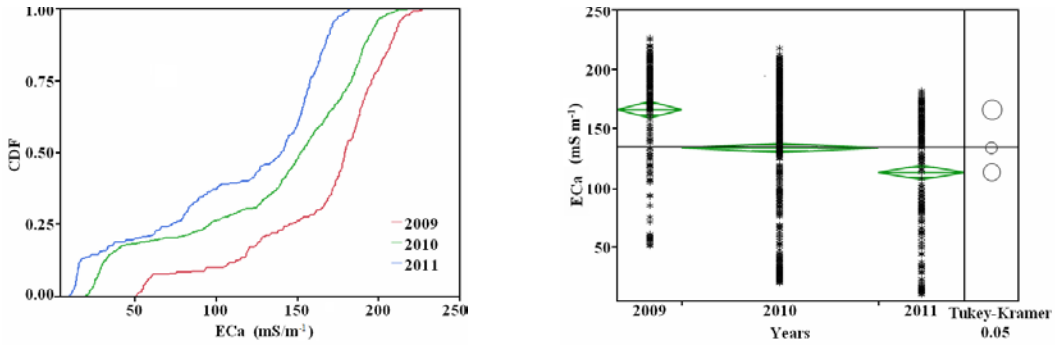

(a) (b)

Fig. 1 (a) Plot of cumulative distribution function (CDF) and (b) One-Way ANONA analysis of ECa

Table 1 Descriptive statistics of ECa (mS m^{-1}) in 2009, 2010 and 2011

Year	n	Mean	Standard error	Min	10%	25%	Median	75%	90%	Max
2009	251	166.19	3.50	51.3	96.28	145.4	179.3	195.6	209.18	226.7
2010	256	134.02	2.00	20.1	29.49	96.15	151.85	182.9	193.4	217.7
2011	339	113.29	3.01	10.5	15.9	73.2	140.2	157.9	168.5	181.8

Table 2 Comparisons for means using the Tukey-Kramer test for ECa (mS m^{-1}) in 2009, 2010 and 2011

Year	Mean	2009	2010	2011
2009	166.19	-11.61	22.71	42.06
2010	134.02		-6.64	12.24
2011	113.29			-9.99

3.2. Spatio-temporal variation of EM38-directed soil salinity

Analyses of spatial dependence were carried out on all the three datasets. The fitted semivariogram models for the EM38 data (ECa) in years 2009-2011 and the parameters for these models are given in Table 3. The semivariogram models of ECa indicate the spatial behavior had good continuity in space and can be modeled quite well with exponential models. However, they display different tendencies. The nugget value (C_0) decreased from 2009 to 2011, indicating the variations in soil salinity are becoming smaller and smaller. The ratios of C_0 to sill ($C+C_0$) decline sharply, from 17.07%

(2009) to 0.26% (2011). According to Shi et al[15], the ratio of C_0 to ($C+C_0$) can be used to denote spatial dependence of soil attributes. In this regard, we can conclude that the autocorrelation of ECa was becoming stronger during our study period, which may be induced by the alternating irrigation and drainage practices necessary for rice cultivation. In addition, the relatively large nugget effect for ECa data is most probably the consequence of uneven distribution of soil salinity between ridge and furrow irrigation, coupled perhaps with a small georeferencing error of EM38 positioning.

Table 3 Models and parameters of semivariogram for ECa (mS m^{-1}) in 2009, 2010 and 2011.

Year	Semivariogram model	Nugget (C_0)	Sill (C_0+C)	$C_0/(C_0+C)$	Range (A)	r^2
2009	Exponent model	495	2899	17.07	225.90	0.964
2010	Exponent model	380	4302	8.83	165.00	0.912
2011	Exponent model	10	3807	0.26	127.50	0.928

Finally, we used kriging interpolation to map the variations of ECa in each of the three years. The smoothed contour maps obtained for the three years are shown in Fig.2a, b and c. As shown in these three maps, the spatial distribution of soil salinity can be easily recognized, which is helpful in management on fertility, and developing and applying agronomic practices. The ordinary kriging maps of each ECa dataset show quite similar patterns with a high ECa level (i.e. >175 mS m^{-1}) in the middle and low ECa levels (i.e. <100 mS m^{-1}) in the surrounding regions. Also, we can observe that the ECa is decreasing with the operation years for all the ECa levels. For example, the maximum value of ECa is 181.8 mS m^{-1} in 2011 versus 226.7 mS m^{-1} in 2009 with the minimum value of ECa also decreasing from 2009 (51.3 mS m^{-1}) to 2011 (10.5 mS m^{-1}). The high ECa level in the middle is mainly induced by agricultural practices, such as tillage by large-size tractor (which tends to result in uniform field surface topography), irrigation and drainage for rice cultivation which leach the soil salt into deeper soil layers; and soil salt migration with the water table to topsoil, ditches, and channels around the field. The low ECa level in the surrounding field may arise of the drainage ditches surrounded the field, the same-continuous agricultural practices (i.e. ridge building in the surroundings, irrigation and drainage for rice) make the soil salinity content become lower in surroundings. Water table fluctuations are also mitigated by the presence of drainage ditches with an approximate depth of 0.8 m and as such, the topsoil and subsoil ECa gradually declines.

In order to assess temporal stability, we calculated the coefficient of variation (CVt_i) over time at each measurement to assess the stability of soil salinity by ECa, and Fig. 2d shows the CVt_i for every ECa survey location. In this regard, we consider the variation is stable with CVt_i <10%, and is moderately stable with 10% < CVt_i <25%, and unstable 25% < CVt_i <100% according to Shi et al[15]. Interestingly, it can be found that the middle region with a high salinity content (ECa) displayed temporal stability, versus the surrounding region with a lower salinity level (ECa) showed temporal instability. It is not readily apparent why these performances occurred and this matter still needs further investigation and analysis.

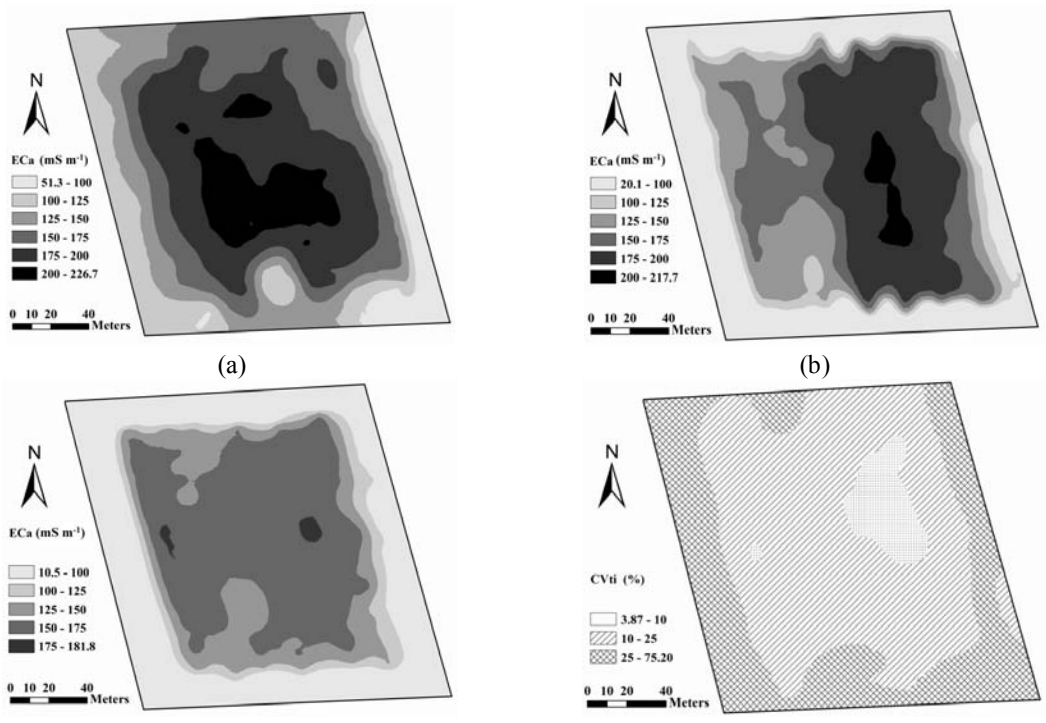

Fig. 2 Spatial variability of ECa in 2009 (a), 2010 (b) and 2011(c) with the plot of (d) coefficient of variation (CVt_i) over time

4. Conculusions

Variability in the soil body calls for fine-scale description, both in space and time. In the present study, the measurement is conducted in the coastal saline areas soil salinity is the key factor that affects the measurements in saline areas or similar saline-sodic soil. We found that the variation of ECa can successfully interpret the spatial variability of soil salinity by (geo)statistics analysis. The significant correlation relationship between ECa and EC1:5 (i.e. R^2 >0.9) allowed us to find that ECa can be used to characterize the spatio-temporal variability of soil salinity. The analyses of the spatial distribution and trend maps revealed the relatively high salinity in the middle, which can be explained by farming and water table fluctuation. And, low soil salinity in the surroundings may arise of the drainage ditches surrounded the field (i.e. ridge building in the surroundings, irrigation and drainage for the rice). In addition, soil salinity decreased from 2009 to 2011 with continued crop cultivation. This conclusion is of importance to farmers who can take measures to decrease soil salinity content for high crop productivity and sustained economic return. As such, we mapped the temporal stability middle region with a high salinity content (ECa) displayed temporal stability, versus the surrounding region with a lower salinity level (ECa) showed temporal instability. These case study results confirm that soil salinity substantially changes with the tillage years and the agricultural practices used in rice paddy fields. This may be due to rice planting with continuous irrigation and drainage. In regards to other crop types, we will verify it in future research. In addition, our findings deepen the understanding of how salinity changes with time, allow us to better understand the influence of these changes on crops in various conditions, and can direct soil sampling strategies.

Acknowledgements

This article is Supported by the National Key Technologies R&D Program of China (No. 2011BAD21B04), National Natural Science Foundation of China (No. 41271234) and the Key National Projects of High-Resolution Earth Observing System (09-Y30B03-9001-13/15).

References

[1] R. A. Viscarra Rossel, A. B. McBratney, and B. Minasny, "*Proximal Soil Sensing*". Netherlands, Springer Science+Business Media B. V., 2010.

[2] D. B. Myers, N. R. Kitchen, K. A. Sudduth, S. Grunwald, R. J. Miles, E. J. Sadler, and R. P. Udawatta, "Combining proximal and penetrating soil electrical conductivity sensors for high-resolution digital soil mapping", in R. A. Viscarra Rossel, A. B. Bratney, and B. Minasny (eds.), *Proximal Soil Sensing*, Netherlands, Springer Science+Business Media B. V., 2010, pp. 233-243.

[3] S. Gmur, D. Vogt, D. Zabowski, and L.M. Moskal, "Hyperspectral analysis of soil nitrogen, carbon, carbonate, and organic matter using regression trees", *Sensors*, *Volume* 3, 2012, pp. 10639-10658.

[4] S. O. Chung, A. K. Sudduth, and J. W. Hummel, "Design and validation of an on-the-go soil strength profile sensor", *Trans. Am. Soc. Agric. Biol. Eng. Volume* 49, 2006, pp. 5-14.

[5] A. B. Loreto, and M. T. Morgan, "Development of an automated system for field measurement of soil nitrate", Paper No. 96-1087. *ASAE*, St Joseph, Michigan, 1996.

[6] J. Triantafilis, G. M. Laslett, and A. B. McBratney, "Calibrating an electromagnetic induction instrument to measure salinity in soil under irrigated cotton", *Soil Sci. Soc. Am. J. Volume* 64*,* 2000, pp. 1009-1017.

[7] S. M. Lesch, D. L. Corwin, and D. A. Robinson, "Apparent soil electrical conductivity mapping as an agricultural management tool in arid zone soils", *Comput. Electron. Agri. Volume* 46, 2005, pp. 351-378.

[8] F. J. Moral, J. M. Terrón, and J. R. Marques da Silva, "Delineation of management zones using mobile measurements of soil apparent electrical conductivity and multivariate geostatistical techniques", *Soil Till. Res. Volume* 106, 2010, pp. 335-343.

[9] Y. Guo, Z. Shi, H. Y. Li, and J. Triantafilis, "Application of digital soil mapping methods for identifying salinity management classes based on a study on coastal central China", *Soil Use Manage. Volume* 29**,** 2013, pp. 445-456.

[10] A. Douaik, M. Van Meirvenne, a nd T. Tóth, "Soil salinity mapping using spatio-temporal kriging and Bayesian maximum entropy with interval soft data", *Geoderma Volume* 128, 2005, pp. 234-248.

[11] J. D. McNeill, "Electromagnetic Terrain Conductivity Measurement at Low Induction Numbers: Technical Note TN-6", GEONICS Limited, Ontario, Canada, 15. 1980.

[12] R. Webster, and M. A. Oliver, "Geostatistics for Environmental Scientists". England, John Wiley & Sons, 2007.

[13] S. Blackmore, "The interpretation of trends from multiple yield maps", *Comput. Electro. Agr. Volume* 26, 2000, pp. 37-51.

[14] Z. Shi, K. Wang, J. S. Bailey, C. Jordan, and A. H. Higgins, "Temporal changes in the spatial distribution of some soil properties on a temperate grassland site" *Soil Use Manage. Volume* 18, 2002, pp. 353-362.

[15] Z. Shi, Y. Li, R. C. Wang, and F. Makeschine, "Assessment of temporal and spatial variability of soil salinity in a coastal saline field", *Environ. Geol. Volume* 48, 2005, pp.171-178.